Synthesis and Characterization of Two Novel Mesolamellar Aluminophosphates

Yaroslav Z. Khimyak and Jacek Klinowski*

Department of Chemistry, University of Cambridge, Lensfield Road, Cambridge CB2 1EW, U.K.

Received March 26, 1998. Revised Manuscript Received May 29, 1998

Two new mesolamellar aluminophosphates, designated L1 and L2, have been synthesized by supramolecular templating from aqueous solutions containing a cationic surfactant and tetraalkylammonium hydroxide. The structure, morphology, and properties of the products have been examined by XRD, SEM, solid-state NMR, thermogravimetry and FTIR, and optimal synthesis conditions have been established. Although the compositions of the starting mixtures for the synthesis of L1 and L2 are similar, the structures of the two materials are different. In L2 phosphorus is coordinated to four AlO_4 tetrahedra; this is the most significant difference between the two products, responsible for the higher thermal stability of L2. The synthesis of L2 requires higher temperatures than that of L1.

Introduction

The discovery of mesoporous silica molecular sieves, formed through structure-directing interaction of surfactant micelles with inorganic precursors[1,2] has expanded the range of silica-based materials available for various heterogeneous processes with the participation of relatively large organic molecules and as hosts for supramolecular assembly. The supramolecular templating pathway has been applied for the synthesis of various inorganic−organic composites. Heteroatom-modified mesoporous silicate molecular sieves with hexagonal and cubic pore arrangements (MCM-41 and MCM-48, respectively)[3−8] and numerous metal oxide mesocomposites have been obtained using both cationic and neutral surfactants.[9−14]

Some aluminophosphates and related materials are useful as catalysts and sorbents.[15−18] The fact that $AlPO_4$ and silica are isostructural suggests that materials with structures analogous to those of mesoporous silicates can also be obtained in the aluminophosphate system.[19−23] The use of long-chain amines as structure-directing templates leads to the formation of lamellar aluminophosphates, both from aqueous and nonaqueous media. The Al:P ratio in the materials reported in the literature varies from 2:1 to 1:2, and their structure and properties depend on the synthetic procedure.[24−26]

The cationic templating pathway using quaternary ammonium surfactants has led to a number of phosphate-based materials. Lamellar zinc phosphates have been prepared using cationic surfactants via the $S^+X^-I^+$ templating pathway. At least four lamellar $C_nH_{2n+1}N(CH_3)_3{}^+X^-(HZnPO_4)$ (where X = Cl, Br) phases, with different *d* spacings and surfactant packing, including monolayer and bilayer geometry, have been synthesized

(1) Beck, J. S.; Vartuli, J. C.; Roth, W. J.; Leonowicz, M. E.; Kresge, C. T.; Schmitt, K. D.; Chu, C. T. W.; Olson, D. H.; Sheppard, E. W.; McCullen, S. B.; Higgins, J. B.; Schlenker, J. L. *J. Am. Chem. Soc.* **1992**, *114*, 10834.
(2) Kresge, C. T.; Leonowicz, M. E.; Roth, W. J.; Vartuli, J. C.; Beck, J. S. *Nature* **1992**, *359*, 710.
(3) Sayari, A.; Moudrakovski, I.; Danumah, C.; Ratcliffe, C. I.; Ripmeester, J. A.; Preston, K. F. *J. Phys. Chem.* **1995**, *99*, 16373.
(4) Luan, Z. H.; Cheng, C. F.; Zhou, W. Z.; Klinowski, J. *J. Phys. Chem.* **1995**, *99*, 1018.
(5) Alba, M. D.; Luan, Z. H.; Klinowski, J. *J. Phys. Chem.* **1996**, *100*, 2178.
(6) Kim, J. B.; Inui, T. *Catal. Lett.* **1996**, *36*, 255.
(7) Hartmann, M.; Poppl, A.; Kevan, L. *J. Phys. Chem.* **1995**, *99*, 17494.
(8) Schmidt, R.; Junggreen, H.; Stocker, M. *J. Chem. Soc., Chem. Commun.* **1996**, 875.
(9) Huo, Q. S.; Margolese, D. I.; Ciesla, U.; Demuth, D. G.; Feng, P. Y.; Gier, T. E.; Sieger, P.; Firouzi, A.; Chmelka, B. F.; Schüth, F.; Stucky, G. D. *Chem. Mater.* **1994**, *6*, 1176.
(10) Vaudry, F.; Khodabandeh, S.; Davis, M. E. *Chem. Mater.* **1996**, *8*, 1451.
(11) Ulagappan, N.; Rao, C. N. R. *J. Chem. Soc., Chem. Commun.* **1996**, 1685.
(12) Ciesla, U.; Demuth, D.; Leon, R.; Petroff, P.; Stucky, G.; Unger, K.; Schüth, F. *J. Chem. Soc., Chem. Commun.* **1994**, 1387.
(13) Antonelli, D. M.; Ying, J. Y. *Angew. Chem., Int. Ed. Engl.* **1995**, *34*, 2014.
(14) Antonelli, D. M.; Ying, J. Y. *Chem. Mater.* **1996**, *8*, 874.
(15) Szostak, R. *Molecular Sieves. Principles of Synthesis and Identification*; Van Nostrand Reinhold: New York, 1989.
(16) Eder, F.; Lercher, J. A. *J. Phys. Chem.* **1996**, *100*, 16460.
(17) Akolekar, D. B.; Huang, M.; Kaliaguine, S. *Zeolites* **1994**, *14*, 519.
(18) Lee, Y. J.; Chon, H. *J. Chem. Soc., Faraday Trans.* **1996**, *92*, 3453.
(19) Wilson, S. T.; Lok, B. M.; Messina, C. A.; Cannan, T. R.; Flanigen, E. M. *J. Am. Chem. Soc.* **1982**, *104*, 1146.
(20) Dessau, R. M.; Schlenker, J. L.; Higgins, J. B. *Zeolites* **1990**, *10*, 522.
(21) Davis, M. E.; Saldarriaga, C.; Montes, C.; Garces, J.; Crowder, C. *Nature* **1988**, *331*, 698.
(22) Estermann, M.; McCusker, L. B.; Baerlocher, C.; Merrouche, A.; Kessler, H. *Nature* **1991**, *352*, 320.
(23) Gao, Q. M.; Li, S. G.; Xu, R. R.; Yue, Y. *J. Mater. Chem.* **1996**, *6*, 1207.
(24) Oliver, S.; Kuperman, A.; Coombs, N.; Lough, A.; Ozin, G. A. *Nature* **1995**, *378*, 47.
(25) Sayari, A.; Moudrakovski, I.; Reddy, J. S.; Ratcliffe, C. I.; Ripmeester, J. A.; Preston, K. F. *Chem. Mater.* **1996**, *8*, 2080.
(26) Gao, Q. M.; Chen, J. S.; Xu, R. R.; Yue, Y. *Chem. Mater.* **1997**, *9*, 457.

S0897-4756(98)00708-X CCC: $15.00
Published on Web 07/30/1998

by controlling the pH and gel composition.[27] The synthesis of hexagonal mesostructured materials based on vanadium(V)−phosphorus oxide with V:P = 2 has been reported, but removal of the template by calcination at 773 K causes structural collapse.[28]

We have used the cationic templating pathway to synthesize aluminophosphate mesocomposites from aqueous solutions. Two distinctly different materials, designated L1 and L2, have been obtained from starting mixtures with slightly different chemical compositions. The differences between CTAC−AlPO mesocomposites have been monitored by powder X-ray diffraction (XRD), solid-state NMR, FTIR, TGA, and SEM. Layered aluminophosphates can be prepared under similar reaction conditions in nonaqueous systems.[29−34] Similar regularities apply in syntheses without an organic solvent. Hexagonal aluminophosphate[35,36] and silicoaluminophosphate[37] mesocomposites have also been reported.

Although formation of many mesolamellar surfactant−metal oxide materials has been reported, we have found that, uniquely, the cationic templating pathway gives two aluminophosphates with different connectivities in the inorganic framework but the same arrangement of the organic component.

Experimental Section

Synthesis. In a typical synthetic procedure the appropriate amount of aluminum triisopropoxide (Aldrich, 98%) was mixed with water (molar ratio $H_2O:Al_2O_3 = 65$) under vigorous stirring. An 85% solution of phosphoric acid (Aldrich) was then added dropwise under stirring into the homogeneous slurry. The resultant mixture was homogenized by stirring for 45−60 min. Depending on the water content of the starting mixture, the aluminophosphate mixture was diluted with water and stirred for an additional 15 min. Finally, a solution of CTAC (cetyltrimethylammonium chloride) and (TMA)OH (tetramethylammonium hydroxide) (both from Aldrich) was added dropwise to the mixture, which was then stirred for 1 h. The final mixture was transferred into a Teflon-lined stainless steel autoclave and heated at various temperatures in the 80−150 °C range under autogenous pressure for 24−96 h. The reaction was arrested by quenching the autoclave with cold water, and the precipitates were collected, washed with water, and dried at 50 °C overnight. CTAC/OH used in some syntheses was obtained by the batch ion exchange of an aqueous solution of CTAC using the OH-functionalized IRA-440 ion-exchange resin (Aldrich).

Powder XRD. XRD patterns were recorded using a Philips 1710 powder diffractometer with Cu Kα radiation (40 kV, 40 mA), 0.020° step size, and 0.5−2.0 s counting time per step.

Solid-State NMR. NMR spectra were recorded at 9.4 T on a Chemagnetics CMX-400 spectrometer with zirconia rotors 4 mm in diameter spun in air at 4−8 kHz.[27] Al magic angle spinning (MAS) NMR spectra were acquired at 104.20 kHz with less than $\pi/10$ pulses (pulse length, 0.2 μs). A set of 500 scans was acquired with a recycle time of 0.3 s. Cross-polarization (CP) $^1H-^{27}Al$ MAS NMR spectra were measured with a single contact pulse sequence with MAS at 4 kHz, 1 ms contact time, 4.60 μs ^1H $\pi/2$ pulse, 4 s recycle time, and 400 acquisitions. The Hartmann−Hahn condition was established on a sample of kaolinite. The position of ^{27}Al resonances is quoted in parts per million from external $[Al(H_2O)_6]^{3+}$.

^{31}P MAS NMR spectra were measured at 161.885 kHz with MAS at 8 kHz, $\pi/2$ pulses (pulse length 2.50 μs), 8 scans, and 60 s recycle delays. $^1H-^{31}P$ CP/MAS spectra were recorded with a single contact time scheme with MAS at 8 kHz, 1 ms contact time, 4.20 μs ^1H $\pi/2$ pulse, 4 s recycle time, and 256 acquisitions. The Hartmann−Hahn condition was established using a sample of ammonium dihydrogen orthophosphate. ^{31}P chemical shifts are quoted with respect to external 85% H_3PO_4.

^{13}C CP/MAS spectra with ^1H decoupling were recorded at 100.565 kHz for ^{13}C and 399.899 kHz for ^1H. Decoupling used 2.00 μs pulses, 5 s recycle delays, and 1000 scans. CP spectra were acquired with a single contact sequence and 4 ms contact time, 4.10 μs ^1H $\pi/2$ pulse, 5 s recycle time, and 400 scans. The Hartmann−Hahn condition was established on a sample of hexamethylbenzene. The ^{13}C spectra were recorded with MAS at 4 kHz.

FTIR Measurements. FTIR spectra were recorded on a Nicolet 205 FTIR spectrometer using 200 scans with 2 cm^{-1} resolution. Samples were prepared by the KBr disk technique.

Thermogravimetry. Thermogravimetric analysis was carried out using a Polymer Laboratories TGA 1500 instrument under a flow of nitrogen and with a heating rate of 15 °C/min.

Elemental Analysis. Samples were analyzed for carbon, hydrogen, and nitrogen on a Carlo Erba elemental analyzer. Phosphorus was determined colorimetrically. JEOL 5800 and JEOL 2101 scanning electron microscopes, with energy-dispersive X-ray (EDS) attachments, operating at 15 and 200 kV respectively, were used to determine the P:Al ratio.

Scanning Electron Microscopy. Scanning electron microscopy (SEM) images were obtained using a SM Hitachi S-4100 field emission gun operating at 25 kV.

Results and Discussion

Synthesis. Hydrothermal synthesis in the $Al(OiPr)_3-H_3PO_4-CTAC-(TMA)OH-H_2O$ system gives mesolamellar aluminophosphates L1 and L2 with $d_{001}(L1) < d_{001}(L2)$ (Figure 1). Amorphous aluminum phosphate and $AlPO_4-H3$[38] can also be formed. To optimize the crystallization conditions of L1 and L2, we have used synthesis mixtures with different $Al_2O_3:P_2O_5$ ratios and different contents of (TMA)OH, water, and the surfactant.

The type of product is determined by the $Al_2O_3:P_2O_5$:(TMA)OH ratio in the synthesis mixture. High concentrations of phosphoric acid combined with low concentrations of the base promote the formation of L2 and $AlPO_4-H3$. Increased (TMA)OH content promotes the formation of L1 (Table 1). The presence of (TMA)OH in the mixture is essential for the mesocomposites to be formed, and the use of NaOH instead of (TMA)OH while maintaining the same pH gave amorphous prod-

(27) Huo, Q. S.; Margolese, D. I.; Ciesla, U.; Feng, P. Y.; Gier, T. E.; Sieger, P.; Leon, R.; Petroff, P. M.; Schüth, F.; Stucky, G. D. *Nature* **1994**, *368*, 317.
(28) Abe, T.; Taguchi, A.; Iwamoto, M. *Chem. Mater.* **1995**, *7*, 1429.
(29) Chippindale, A. M.; Powell, A. V.; Bull, L. M.; Jones, R. H.; Cheetham, A. K.; Thomas, J. M.; Xu, R. R. *J. Solid State Chem.* **1992**, *96*, 199.
(30) Oliver, S.; Kuperman, A.; Lough, A.; Ozin, G. A. *Chem. Mater.* **1996**, *8*, 2391.
(31) Barrett, P. A.; Jones, R. H. *J. Chem. Soc., Chem. Commun.* **1995**, 1979.
(32) Jones, R. H.; Thomas, J. M.; Xu, R. R.; Huo, Q. S.; Cheetham, A. K.; Powell, A. V. *J. Chem. Soc., Chem. Commun.* **1991**, 1266.
(33) Thomas, J. M.; Jones, R. H.; Xu, R. R.; Chen, J. S.; Chippindale, A. M.; Natarajan, S.; Cheetham, A. K. *J. Chem. Soc., Chem. Commun.* **1992**, 929.
(34) Jones, R. H.; Chippindale, A. M.; Natarajan, S.; Thomas, J. M. *J. Chem. Soc., Chem. Commun.* **1994**, 565.
(35) Feng, P. Y.; Xia, Y.; Feng, J. L.; Bu, X. H.; Stucky, G. D. *J. Chem. Soc., Chem. Commun.* **1997**, 949.
(36) Zhao, D. Y.; Luan, Z. H.; Kevan, L. *J. Chem. Soc., Chem. Commun.* **1997**, 1009.
(37) Chakraborty, B.; Pulikottil, A. C.; Das, S.; Viswanathan, B. *J. Chem. Soc., Chem. Commun.* **1997**, 911.
(38) Li, H. X.; Davis, M. E. *J. Chem. Soc., Faraday Trans.* **1993**, *89*, 957.

Table 1. Composition of the Synthesis Mixtures

	molar ratio					mole fraction			
sample no.	Al_2O_3	P_2O_5	(TMA)OH	CTAC	H_2O	Al_2O_3	P_2O_5	(TMA)OH	product
1	1.00	1.50	0.94	2.00	230	0.291	0.436	0.273	H3
2	1.00	1.20	0.60	1.20	132.5	0.356	0.429	0.214	L2+H3
3	0.75	1.00	0.75	1.00	110	0.300	0.400	0.300	L2+H3
4	1.00	1.50	1.17	2.00	230	0.272	0.409	0.319	L2+H3
5	1.00	1.50	1.30	1.00	230	0.263	0.394	0.342	L2+H3
6	1.00	1.70	1.70	1.00	230	0.212	0.362	0.426	L2
7	1.00	1.20	0.92	1.00	230	0.321	0.388	0.291	L2
7a	1.00	1.20	0.92	1.00	132.5	0.321	0.388	0.291	L2
8	1.00	1.00	0.92	1.00	132.5	0.363	0.363	0.273	L2+L1
9	0.90	1.00	0.75	1.00	110	0.339	0.377	0.283	L2+L1
10	1.00	1.20	1.08	1.20	132.5	0.304	0.366	0.330	L2+L1
11	1.00	1.20	1.20	0.80	230	0.293	0.353	0.353	L1
12	1.00	1.00	1.00	0.60	110	0.333	0.333	0.333	L1
13	1.00	1.20	1.33	1.00	230	0.283	0.341	0.375	L1
14	1.00	1.20	1.45	0.80	132.5	0.273	0.330	0.397	L1
15	1.00	1.50	2.00	1.00	230	0.222	0.333	0.445	L1
16	1.00	1.60	2.20	1.00	230	0.208	0.333	0.458	L1

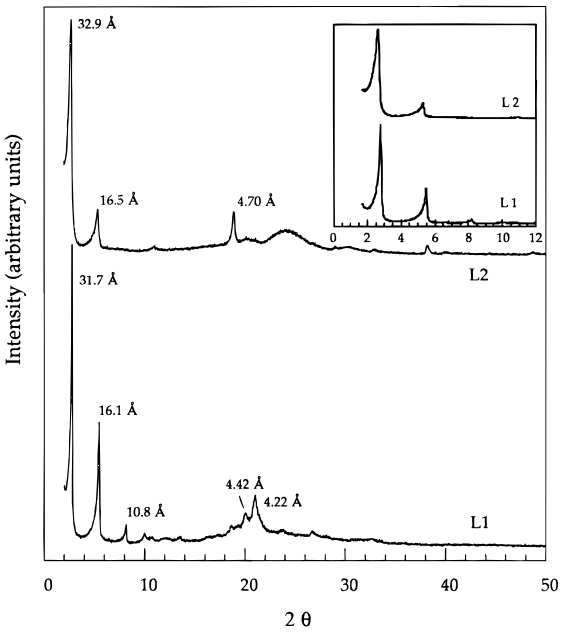

Figure 1. XRD patterns of L1 and L2 synthesized from synthetic mixtures of composition 0.83:1.00:*x*:*y*:*z* Al_2O_3:P_2O_5:CTAC:(TMA)OH:H_2O at 130 °C for 48: h. L1: $x = 0.80$, $y = 1.10$, $z = 190$; L2: $x = 0.60$, $y = 0.75$, $z = 110$.

ucts. On the other hand, both L1 and L2 can be formed using cetyltrimethylammonium hydroxide/chloride obtained by ion exchanging Cl^- by OH^- with the IRA-440 ion-exchange resin. Thus, 45% exchanged (CTA)Cl/OH gave L1 from a mixture of composition 1.0:1.0:2.0:230 Al_2O_3:P_2O_5:(CTA)Cl/OH:H_2O. A mixture of L1 and L2 is obtained when the P_2O_5:Al_2O_3 ratio is increased to 1.20. The fact that the same materials are obtained with CTAC/OH suggests that the key reactions leading to the formation of the mesocomposites take place at the interface between the aggregates of the surfactant and the bulk of the solution. While different mesostructured silicates can be formed from solutions with different surfactant contents,[39,40] only lamellar materials are obtained in the full range of the CTAC content (CTAC:$Al_2O_3 = 0.24-2.00$). However, the concentration of the surfactant controls the degree of crystallinity, and the best quality L1 and L2 are obtained with CTAC:$Al_2O_3 = 0.80-1.00$.

The water content of the synthesis mixture affects the synthesis of L1 to a much greater extent than that of L2 and also affects the structure of the product. Mixtures with lower water contents gave materials (L1a) with a smaller interlayered distance than those for higher water contents (L1b): d_{001}(L1a) = 30.2 Å; d_{001}(L1b) = 31.7 Å. The positions of the two characteristic higher 2θ peaks are 4.42 and 4.22 Å in L1b and 4.32 and 4.09 Å in L1a. Although the ^{27}Al MAS NMR spectra of the products are unaffected by the water content of the synthesis mixture, the ^{31}P spectra show that the two materials are different. The most appropriate temperature for the synthesis of L1 and L2 is 130 °C, and synthesis conducted at the ambient temperature gives amorphous products. However, L1 can be formed at low temperatures (80−130 °C), while high-quality L2 requires much higher temperatures.

X-ray Diffraction. Typical XRD patterns of L1 consist of several peaks (Figure 1). Three peaks in the low-angle region are attributable to the (001), (002), and (003) reflections of the lamellar structure with d_{001}(L1b) = 31.7 Å and d_{001}(L1a) = 30.2 Å. By contrast to the XRD patterns of siliceous mesocomposites which contain only low 2θ reflections, our patterns contain two broad peaks with d_{001} of 4.42 and 4.22 Å for L1b and 4.30 and 4.07 Å for L1a, and several less intense reflections (probably corresponding to impurities) in the 11.0−40.0 2θ range. Inspections of powder patterns show that L1 does not contain dense (cristobalite and tridymite), hydrated (variscite, metavariscite, H2, and H3), or microporous aluminophosphates.

The XRD patterns of L2 mesocomposites are significantly different. The low-angle region contains two intense (001) and (002) reflections. By contrast to the patterns of L1, (003) reflections are absent. We were unable to attribute peaks in the higher 2θ region to impurities. The patterns of numerous samples containing both pure L2 and L2 mixed with $AlPO_4$−H3 or L1 have the same ratios of peak intensities (the intensity of the $d_{002} = 16.5$ Å peak is normally the same as that of the 4.70 Å peak). Higher 2θ peaks are probably related to the arrangement of the layers. Apart from

(39) Huo, Q. S.; Margolese, D. I.; Stucky, G. D. *Chem. Mater.* **1996**, *8*, 1147.
(40) Cheng, C. F.; Zhou, W. Z.; Park, D. H.; Klinowski, J.; Hargreaves, M.; Gladden, L. F. *J. Chem. Soc., Faraday Trans.* **1997**, *93*, 359.

Table 2. Composition of Aluminophosphate Mesocomposites

	synthesis mixture					product			
sample	Al_2O_3	P_2O_5	CTAC	(TMA)OH	H_2O	Al_2O_3	P_2O_5	$(CTA)_2O$	H_2O
L1−1	1.00	1.20	0.96	1.33	230	1.00	1.48	0.505	4.50
L1−2	1.00	1.50	0.96	2.00	230	1.00	1.52	0.537	3.76
L2−1	1.00	1.20	0.72	0.90	132.5	1.00	1.62	0.432	1.94
L2−2	1.00	1.20	0.96	0.90	132.5	1.00	1.67	0.450	2.22

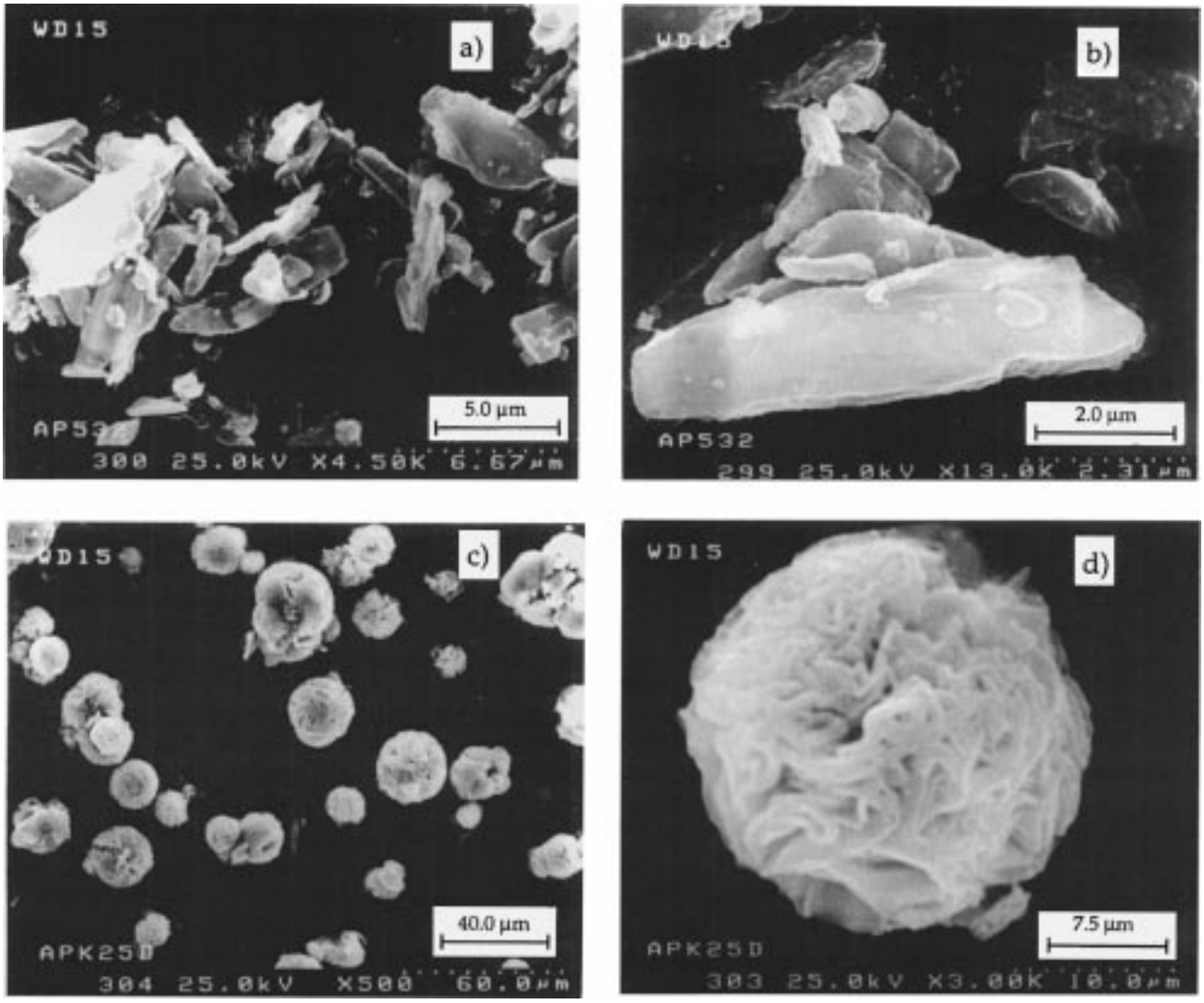

Figure 2. SEM microphotographs of (a−b) L1 and (c−d) L2.

the narrow peaks, XRD patterns of L2 contain broad lines at ca. 20.2, 22.7, and 24.0° 2θ.

Reflections in the 20° region of 2θ in mesolamellar silicates have been attributed to the packing of hydrocarbon chains within the layers.[39] High-angle reflections for $(C_{16}H_{33}N(CH_3)_3Br)(HZnPO_4)$ mesocomposites were found to be related to the internal structure of the layers, and the structure has been indexed to an orthorhombic cell.[9] Very similar high-angle peaks have been reported for hexagonal SAPO synthesized via cationic templating pathway with the presence of CTAB.[37]

Composition. Elemental analysis shows that the C:N atomic ratio in both L1 and L2 is 19.0, the same as in the cetyltrimethylammonium cation, which is therefore the only organic species present. The ^{13}C MAS and CP/MAS NMR spectra are the same as those for $C_{16}H_{33}N(CH_3)_3^+$ in siliceous mesocomposites.[41] The results of elemental analysis are in full agreement with thermogravimetric results. The composition of the highest quality products is given in Table 2. Neither L1 or L2 contain a significant amount of chlorine. The P:Al ratio, determined by EDS, was 3:2 for L1 and 5:3 for L2.

Morphology. SEM microphotographs (Figure 2) show that the L1 mesocomposites form elongated platelets ca. 2.5−7.5 μm long. The morphology of the minor product is irregular. L2 forms spherical aggregates 7.0−26.0 μm in diameter, each consisting of folded aluminophosphate sheets. No other products have been detected.

(41) Wang, L. Q.; Liu, J.; Exarhos, G. J.; Bunker, B. C. *Langmuir* **1996**, *12*, 2663.

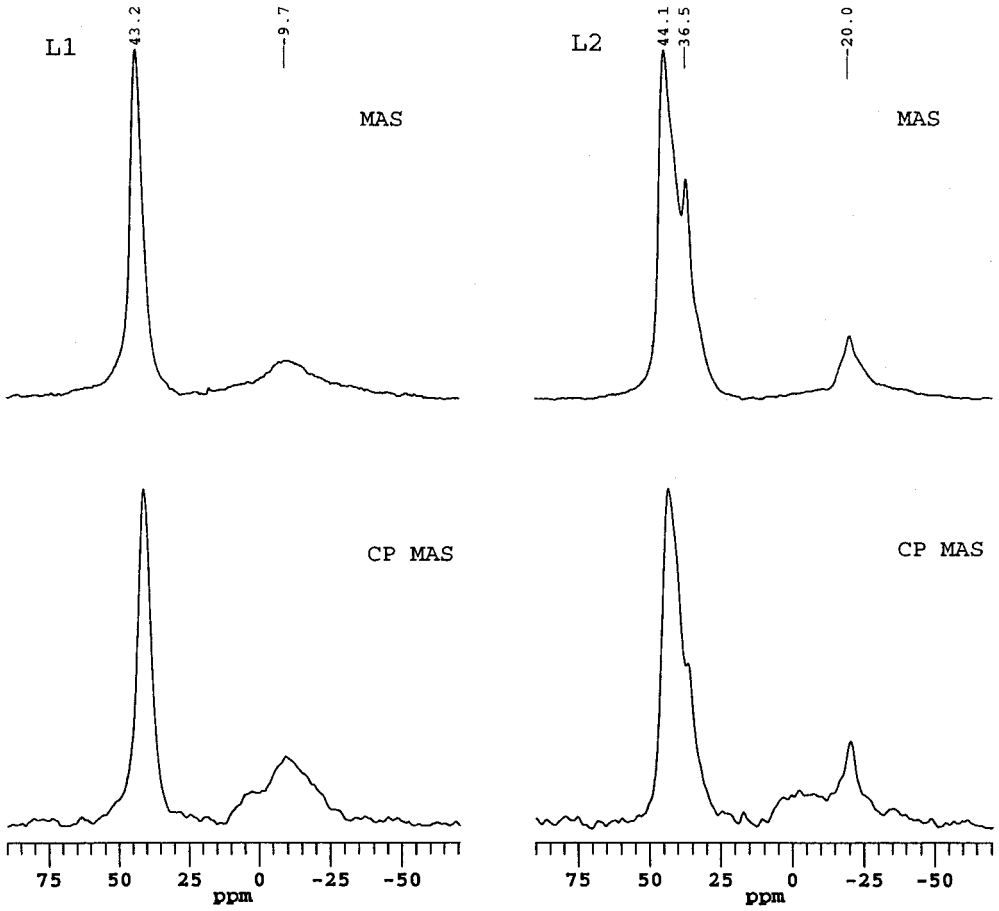

Figure 3. ^{27}Al MAS NMR spectra of L1 and L2.

^{27}Al MAS NMR. Solid-state NMR reveals that the environments of both aluminum and phosphorus in the two products are significantly different. Aluminum is predominantly four-coordinate (tetrahedral) in both materials. The ^{27}Al MAS NMR spectra of L1 contain two main resonances (Figure 3): at 42.8−43.0 ppm (from four-coordinate Al) and between −8.5 and −10.0 ppm (Al six-coordinated to water and/or PO_4 groups). The ^{27}Al spectra of the samples made under various reaction conditions show that the tetrahedral:octahedral ratio is related to the crystallinity of the products: the higher the intensity of the (00*n*) XRD peaks (n = 1, 2, 3), the larger the tetrahedral/octahedral ratio. This suggests that six-coordinate Al is associated with amorphous aluminum phosphate or alumina.

^{27}Al MAS NMR spectra reveal the presence of several inequivalent kinds of aluminum in L2 (Figure 3). The peaks at 44.1 and 36.7 ppm correspond to two different kinds of four-coordinate Al, while the narrow peak at ca. −20.1 ppm comes from six-coordinate Al. The spectra of samples synthesized for 24 h or with an insufficient quantity of the template contain an additional broad peak (at ca. −8.2 to −10.0 ppm) from six-coordinate Al.

The ^{1}H−^{27}Al CP/MAS spectra of L1 show enhancement of the intensity of the line from six-coordinate Al relative to that from four-coordinate Al, which indicates the closeness of Al to H_2O and/or OH. The intensity of the 36.5 ppm line in the CP/MAS spectrum of L2 is reduced with respect to the MAS line at 44.2 ppm. The intensity of the line from six-coordinate Al at ca. −20.0 ppm is not significantly enhanced, indicating that it probably comes from Al linked to six PO_4 groups.

^{31}P MAS NMR. The chemical shifts of the peaks in the ^{31}P MAS NMR spectra of L1 prepared from mixtures with different water contents (Figure 4) indicate tetrahedral coordination of phosphorus atoms in the structure. The broad resonance centered at ca. −13.5 ppm in the spectra of L1a and L1b probably comes from an amorphous impurity. The chemical shift suggests that the phosphorus atoms are each linked, through oxygens, to two aluminum atoms. The two remaining oxygens may be in OH or P═O groups, leading to a structure such as $Al(OP)_4(H_2O)_2$.[42]

The positions of the narrow lines depend on the water content of the sample. Thus the spectrum of L1a contains lines at −17.5 and −21.1 ppm of nearly equal intensities, and the spectra of L1b, lines at −18.1 and −21.4 ppm. The line at −18.1 ppm probably represents two unresolved lines at −17.9 and −19.6 ppm. The ^{1}H−^{31}P CP/MAS spectra support this assumption, revealing enhanced intensity of the lines between −12.8 and −13.2 ppm and at −19.6 ppm and a slight decrease of the ratio of the intensities of peaks at −17.9 and −21.4 ppm (Figure 4). We believe that the resonance at −17.5 ppm in the ^{31}P spectrum of L1a is also composed of overlapping peaks, although the very small chemical shift difference of the overlapping lines and the presence of the broad resonances from an amorphous phase

(42) Rocha, J.; Kolodziejski, W.; He, H. Y.; Klinowski, J. *J. Am. Chem. Soc.* **1992**, *114*, 4884.

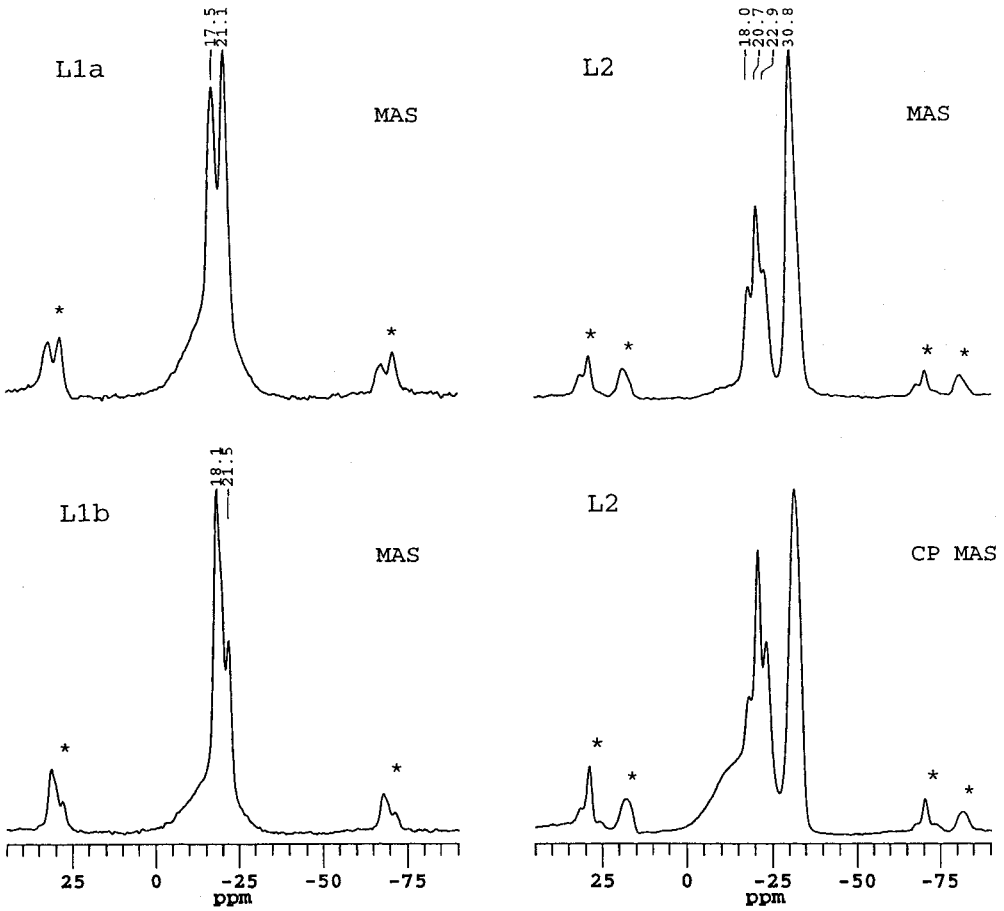

Figure 4. ^{31}P MAS NMR spectra of L1 and L2. Asterisks denote spinning sidebands.

makes spectral analysis difficult. While the ^{31}P spectra of as-synthesized L1a and L1b are different, those of dehydrated samples are identical, with a single resonance at −19.1 ppm. This confirms the structural similarity of the two materials, which differ in the coordination of phosphorus to water.

The main feature of the ^{31}P NMR spectrum of L2 is the dominant peak at −30.7 ppm. The value of the chemical shift suggests that this peak comes from P coordinated to four AlO_4 tetrahedra. Several overlapping peaks are also found (at −13.8, −18.0, −20.5, and −22.8 ppm), all from four-coordinate P, most probably to three Al atoms. The fourth oxygen can be bonded to hydrogen, water, or the surfactant. Close examination of the peak at −30.9 ppm reveals two components at −30.6 and −32.7 ppm. This is confirmed by the spectra of dehydrated L2, where the separation of the two lines is very clear.

The $^{1}H-^{31}P$ CP/MAS spectrum of L2 shows that the peaks between −13.5 and −23.0 ppm have increased in intensity compared with lower field resonances, indicating their involvement in strong P−H dipolar interactions. Also, the spinning sidebands of the peaks between −17.5 and −23.0 ppm are much more intense than those from lines at ca. −30.8 ppm, suggesting a larger chemical shift anisotropy of ^{31}P in the former. However, the overall broadening of the signal in both the MAS and CP/MAS spectra does not permit a precise assignment of the various lines to specific structural units.

The ^{27}Al and ^{31}P spectra of L1 and L2 are significantly different from those reported for mesolamellar aluminophosphates synthesized in the presence of long-chain primary amines,[25,26] which contain a substantial contribution from six-coordinate Al. The ^{31}P chemical shifts in these materials are in the −8.0 to −19.0 ppm range, which excludes P linked to four AlO_4 tetrahedra.

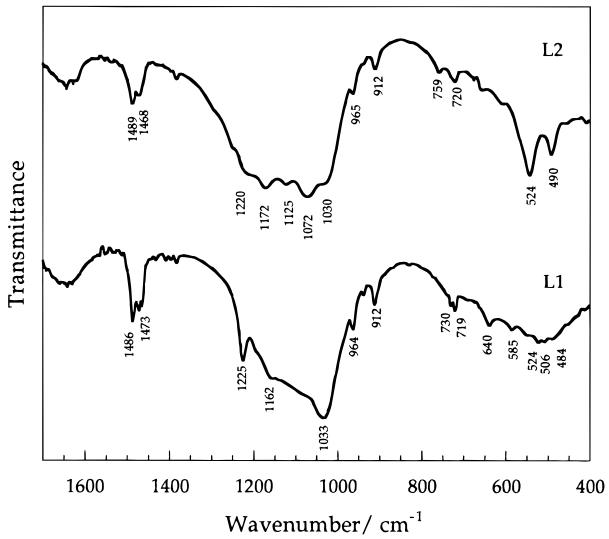

Figure 5. Structural regions of FTIR spectra of L1 and L2.

Infrared Spectroscopy. The FTIR spectra of L1 and L2 (Figure 5) reveal significant differences between the two materials. The spectra of both contain bands at 470−700, 1000−1250, 1610−1670, and 3400−3600 cm^{-1}. Lines attributable to the organic template are also present. The sharp bands at 2917 and 2854 cm^{-1}

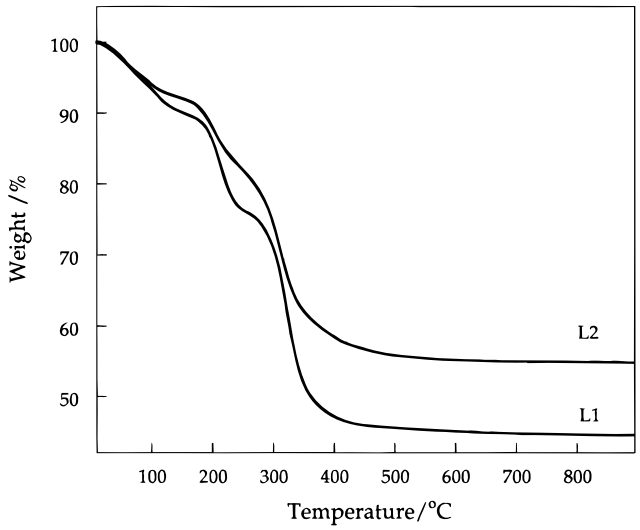

Figure 6. Thermogravimetric curves for L1 and L2 synthesized from mixtures with composition 0.83:1.00:0.60:*y*:*z* Al_2O_3:P_2O_5:CTAC:(TMA)OH:H_2O with $y = 1.10$, $z = 190$ for L1 and $y = 0.75$, $z = 110$ for L2.

correspond to asymmetric and symmetric C−H stretching, respectively. Bands at 1489 and 1460 cm^{-1} are from deformation vibrations, while those at 965−911 cm^{-1} are from skeletal vibrations of the $C-CH_3$ and $C-CH_2-CH_3$ groups. The absorption at 719−725 cm^{-1} comes from skeletal vibrations in the hydrocarbon chains in the surfactant.[43]

The spectra were assigned on the basis of data for microporous $AlPO_4$-*n* materials.[23,44,45] The most significant difference between L1 and L2 is in the structural region of the spectra (400−1650 cm^{-1}). Several bands can be distinguished in the region corresponding to O−T−O asymmetric stretching vibrations. Thus the spectrum of L2 exhibits absorption bands at 1251, 1200, 1172, 1124, 1068, and 1032 cm^{-1}, and the spectrum of L1, at 1225, 1162, 1085, and 1032 cm^{-1}.

The symmetric TO_4 stretching region in the FTIR spectrum of L2 contains weak bands at 660 and 611 cm^{-1} and intense sharp bands at 541 and 472 cm^{-1}. These absorptions either are TO_4 bending vibrations or come from motions of the external linkage of the AlO_4 and PO_4 tetrahedra. The same spectral range in the spectrum of L1 contains sharp bands at 641, 585, 550, 525, 506, and 484 cm^{-1}. Those at 520−641 cm^{-1} are probably symmetric stretching vibrations, and the lower frequency bands, TO_4 bending.

Thermal Stability. Three distinct thermal events can be identified during the decomposition of both L1 and L2 (Figure 6). The loss of water occurs at ca. 100 °C. The second and third steps are at ca. 200 and 320 °C (corresponding to the DTG maxima at 204−209 and 309−315 °C, respectively). As elemental analysis shows that cetyltrimethylammonium cations are the only organic species present, these thermal events must come from a two-stage degradation of the template, although it is possible that the second step is partly related to the loss of interlamellar water.

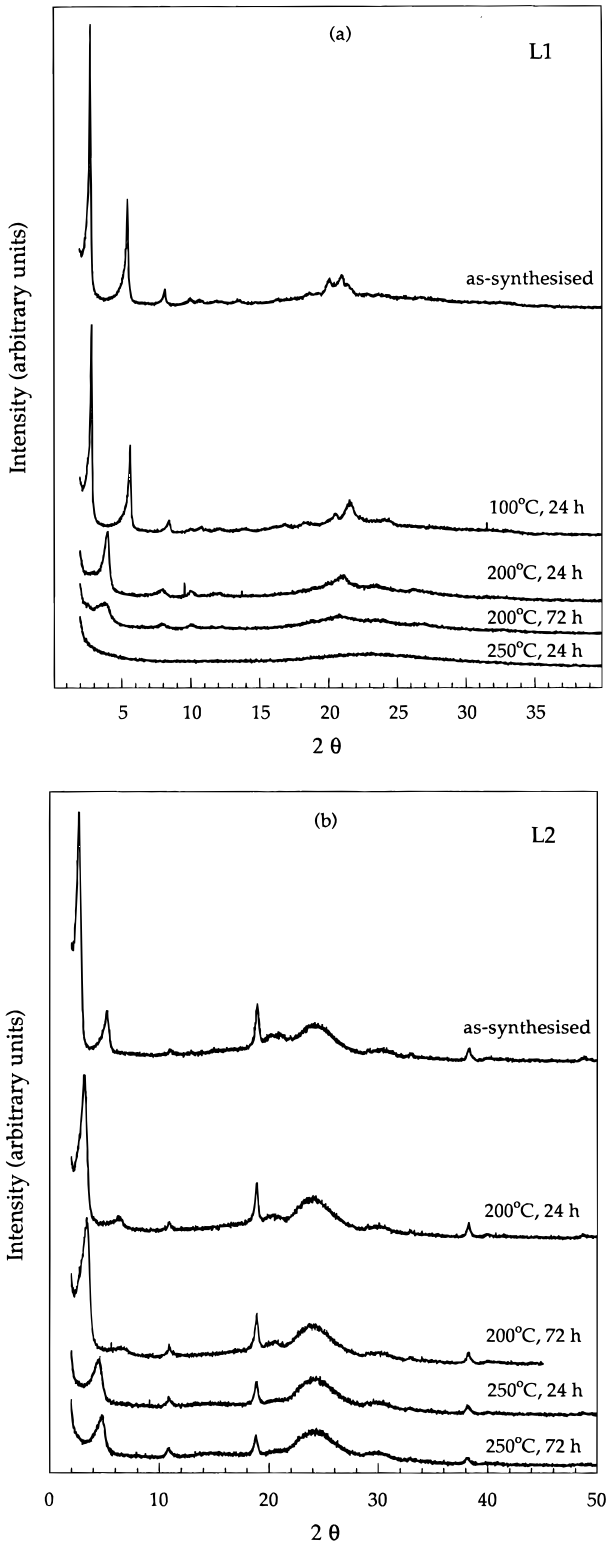

Figure 7. Effect of calcination on the XRD patterns of (a) L1 and (b) L2.

TGA of the L1 and L2 samples prepared from mixtures with various surfactant concentrations shows that in both cases the increase of CTAC content in the solution leads to the rise of the weight loss corresponding to the first and second step in the TG curves. Comparison of TG curves of L1 and L2 materials obtained from the starting mixtures with the same surfactant content shows that, generally, L1 materials contain more water and organic template. The shape

(43) Socrates, G. *Infrared Characteristic Groups Frequencies: Tables and Charts*; Wiley: Chichester, U.K., 1994.
(44) Davis, M. E.; Montes, C.; Hathaway, P. E.; Arhancet, J. P.; Hasha, D. L.; Garces, J. M. *J. Am. Chem. Soc.* **1989**, *111*, 3919.
(45) Stein, A.; Wehrle, B.; Jansen, M. *Zeolites* **1993**, *13*, 291.

of the TG and DTG curves allows us to asses the rate of decomposition of the investigated materials. Thus, the second and third steps in the L1 TG curve are well-separated by the plateau at 240−270 °C. The rate of weight loss during the second step in the TG curve of high-quality L1 materials is usually higher than 0.25 wt %/°C (15 °C/min heating rate). The same parameter for the L2 TG curve is less than 0.18 wt %/°C, showing higher thermal stability of the L2 mesocomposite in comparison with the L1. Not surprisingly, the L1 and L2 materials do not preserve their layered structure upon calcination above 350 °C. Structural changes upon calcination in air at different temperatures have been studied by XRD and solid-state NMR.

Dehydration at 100 °C does not influence the appearance of the XRD pattern. Calcination at 200 °C for 24 h results in the formation of material with a smaller interlamellar distance: 27.62 Å in comparison with 32.97 Å for the as-prepared L2. Calcination for an additional 48 h leads to a slight reduction of d_{100} to 26.22 Å (Figure 7). The peaks at higher 2θ remain unchanged, which indicates that the internal structure of the L2 layers is unaffected by calcination at 200 °C. The XRD patterns of L2 calcined at 250 °C reveal a further decrease of the interlayered distance to 19.0 Å after 24 h of thermal treatment and to 18.46 Å after 72 h. The intensity of the high 2θ peaks also decreases. The lamellar mesostructure collapses completely upon calcination at 320 °C.

Analogous experiments with L1 confirm its lower thermal stability in comparison with L2. Dehydrated L1a and L1b give identical XRD patterns. Calcination at 200 °C for 24 h gives a layered product with d_{001} only 67% of that of as-prepared material (21.38 Å compared with 31.57 Å for L1b; Figure 7). The crystallinity of this product greatly decreases after 72 h of calcination, while the interlamellar distance remains practically unchanged. In contrast to L2, calcination at 250 °C causes a complete collapse of the structure and the formation of an amorphous product.

Acknowledgment. We are grateful to Professor J. Rocha for the SEM images, to Mrs. K. Butler for help with elemental analysis, and to the Cambridge Overseas Trust, Tate & Lyle, and the Cambridge Oppenheimer Fund for financial support.

CM9807081